

Ghoshal-like test of equilibration in near-Fermi-energy heavy-ion collisions

J. Wang,^{1,*} T. Keutgen,^{1,†} R. Wada,¹ K. Hagel,¹ Y. G. Ma,^{1,‡} M. Murray,^{1,§} L. Qin,¹ P. Smith,¹ J. B. Natowitz,¹ R. Alfaro,² J. Cibor,³ A. Botvina,¹ M. Cinausero,⁴ Y. El Masri,⁵ D. Fabris,⁶ A. Keksis,¹ S. Kowalski,⁷ M. Lunardon,⁶ A. Makeev,¹ N. Marie,^{1,¶} E. Martin,¹ Z. Majka,⁸ A. Martinez-Davalos,² A. Menchaca-Rocha,² G. Nebbia,⁶ S. Moretto,⁶ G. Prete,⁴ V. Rizzi,⁴ A. Ruangma,¹ D. V. Shetty,¹ G. Souliotis,¹ P. Staszal,⁸ M. Veselsky,¹ G. Viesti,⁶ E. M. Winchester,¹ S. J. Yennello,¹ and W. Zipper⁷

(NIMROD Collaboration)

¹*Cyclotron Institute, Texas A&M University, College Station, Texas 77843, USA*²*Instituto de Fisica, Universidad Nacional Autonoma de Mexico, Apacado Postal 20-364 01000, Mexico City, Mexico*³*Institute of Nuclear Physics, ul. Radzikowskiego 152, PL-31-342 Krakow, Poland*⁴*INFN, Laboratori Nazionali di Legnaro, I-35020 Legnaro, Italy*⁵*FNRS and IPN, Université Catholique de Louvain, B-1348 Louvain-Neuve, Belgium*⁶*INFN and Dipartimento di Fisica dell' Università di Padova, I-35131 Padova, Italy*⁷*Institute of Physics, University of Silesia, PL-40007, Katowice, Poland*⁸*Jagellonian University, M Smoluchowski Institute of Physics, PL-30059, Krakow, Poland*

A. Ono

Department of Physics, Tohoku University, Sendai 980-8578, Japan

(Received 23 December 2004; published 31 May 2005)

Calorimetric and coalescence techniques have been employed to probe equilibration for hot nuclei produced in heavy-ion collisions of 35 to 55 MeV/nucleon projectiles with medium mass targets. Entrance channel mass asymmetries and energies were selected so that very hot composite nuclei of similar mass and excitation would remain after early stage preequilibrium particle emission. Intercomparison of the properties and deexcitation patterns for these different systems provides evidence for the production of hot nuclei with decay patterns relatively independent of the specific entrance channel.

DOI: 10.1103/PhysRevC.71.054608

PACS number(s): 25.70.Pq, 24.60.Ky, 05.70.Jk

I. INTRODUCTION

Determining the extent to which the properties and subsequent deexcitation of an excited nucleus depend on the entrance channel characteristics of the collision used to prepare that nucleus is a time honored way of exploring equilibration in nuclear systems. In the early, low energy, experiments of Ghoshal [1], indications that the decay of identical compound nuclei, produced at the same excitation energy in reactions induced by protons and alpha particles was independent of the entrance channel provided very strong evidence for the validity of the independence hypothesis [2,3], in statistical decay theories. In higher energy collisions at near-Fermi energies, in which faster emission processes remove energy and mass and the subsequent composite nucleus undergoes some dynamic evolution prior to a possible equilibration, the establishment of equilibration and entrance channel independence is more difficult. Nevertheless, it is precisely in this domain that nuclei are being investigated to determine whether their disassembly

modes are dynamically or thermodynamically driven and, in the latter case, whether they provide evidence of liquid-gas phase changes and critical behavior common to other liquids [4–7]. Tests of the degree of equilibration achieved in these Fermi energy collisions are clearly of interest.

In this article we report on a Ghoshal-like test of the equilibration of medium mass hot composite nuclei produced in central collisions of 35 MeV/nucleon $^{64}\text{Zn} + ^{92}\text{Mo}$, 40 MeV/nucleon $^{40}\text{Ar} + ^{112}\text{Sn}$ and 55 MeV/nucleon $^{27}\text{Al} + ^{124}\text{Sn}$ and in midcentral collisions of 47 MeV/nucleon $^{64}\text{Zn} + ^{92}\text{Mo}$. Correlations between ejectile energy and emission time predicted by AMD-V transport model calculations [8–10] were employed to follow the evolution of the temperatures from the time of first particle emission to the time of equilibration. The early temperature evolutions for the four different systems show a close correspondence although the time range for the observed evolution varies somewhat with reaction system. A very similar double isotope ratio temperature, $T_{\text{HHe}} \sim 6$ MeV, is reached at the end of the preequilibrium stage of each reaction. The average masses and excitation energies remaining at the end of the preequilibrium stage were determined using calorimetric techniques. The derived masses range from 85 to 114 amu and the excitation energies range from 4.88 to 5.31 MeV/nucleon. Comparisons of the subsequent evaporation spectra and particle multiplicities for the four systems provide strong evidence that the deexcitation cascades for these systems are very much alike. The combined results indicate that very similar equilibrated hot nuclei are produced in the four different collisions.

*E-mail address: wang@comp.tamu.edu

[†]Now at FNRS and IPN, Université Louvain-Neuve, Belgium Catholique de Louvain, B-1348 Belgium.[‡]On leave from Shanghai Institute of Nuclear Research, Chinese Academy of Sciences, Shanghai 201800, China.[§]Now at University of Kansas, Lawrence, Kansas 66045-7582.[¶]Now at LCP Caen, ISMRA, IN2P3-CNRS, F-14050 Caen, France.

II. EXPERIMENT

The reactions 35 MeV/nucleon $^{64}\text{Zn} + ^{92}\text{Mo}$, 40 MeV/nucleon $^{40}\text{Ar} + ^{112}\text{Sn}$, 55 MeV/nucleon $^{27}\text{Al} + ^{124}\text{Sn}$, and 47 MeV/nucleon $^{64}\text{Zn} + ^{92}\text{Mo}$ were studied at the K-500 superconducting cyclotron facility at Texas A&M University. The first three reaction systems were selected because various model calculations predict that central collisions lead, after preequilibrium emission, to hot nuclei with very similar composite masses and excitation energies. The $^{27}\text{Al} + ^{124}\text{Sn}$ reaction has a significantly different N/Z ratio than the first two reactions. For the fourth reaction, 47 MeV/nucleon $^{64}\text{Zn} + ^{92}\text{Mo}$, selection of midcentral collisions was predicted to lead to a composite system of comparable energy and mass to those of the central collisions for the first three systems.

For these studies we used the NIMROD detector array that consists of a 4π charged particle array inside a 4π neutron calorimeter. The charged particle detector array of NIMROD includes 166 individual CsI detectors arranged in 12 rings in polar angles from $\sim 4^\circ$ to $\sim 160^\circ$. In these experiments each forward ring included two “super-telescopes” composed of two Si detectors and seven Si-CsI telescopes to identify intermediate mass fragments (IMF). The NIMROD neutron ball, which surrounds the charged particle array, was used to determine the neutron multiplicities by thermalization and capture of emitted neutrons. As the neutron ball provides little neutron energy or angle information, in this experiment we also employed five discrete liquid scintillator neutron detectors of the Belgian-French DEMON array [11] to obtain neutron energy and angular distributions by time of flight techniques. These neutron detectors were placed at laboratory angles of 30° to 110° relative to the beam direction and at distances of 2 to 3 ms from the target. For these measurements the top quadrant of the midsection of the neutron ball was raised to allow 5-cm gaps between neighboring sections. The DEMON detectors viewed the target through one of these gaps. Given the large amount of material in the NIMROD detector, this configuration is not ideal for measurements of discrete neutron spectra. However, the neutron ball is a very effective absorber for scattered neutrons. By employing a standard reaction, 26 MeV/nucleon $^{40}\text{Ar} + ^{92}\text{Mo}$, for which neutron spectra and multiplicities have previously been well established by Yoshida *et al.* [12], we empirically determined the required DEMON detector efficiency curves appropriate to our experimental configuration. Much greater detail on the detection systems and calibrations may be found in Refs. [9,11].

During the experiment, data were taken employing two different trigger modes. One was a minimum bias trigger in which at least one of the CsI detectors detected a particle. The other was a high multiplicity trigger that required detected particles in three to five CsI detectors (depending on the reaction studied).

III. DATA ANALYSIS

Many of the techniques applied in this analysis have been discussed previously in greater detail in references [9,10,13–16]. Only a brief summary of these techniques is included in the present work.

An inspection of the two dimensional arrays depicting the detected correlation between charged particle multiplicity and neutron multiplicity in NIMROD (not shown), reveals a distinct correlation in which increasing charged particle multiplicity is associated with increasing neutron multiplicity. Although there are significant fluctuations reflecting both the competition between the different decay modes and the detection efficiencies, these correlations provide a means for selecting the most violent collisions. For the analysis reported in this article we have selected events corresponding to the largest observed neutron and charged particle multiplicities. For 35 MeV/nucleon $^{64}\text{Zn} + ^{92}\text{Mo}$, 40 MeV/nucleon $^{40}\text{Ar} + ^{112}\text{Sn}$, and 55 MeV/nucleon $^{27}\text{Al} + ^{124}\text{Sn}$, the 10% highest multiplicity events taken with the minimum bias trigger were selected in this manner. This selection emphasizes the lower impact parameter collisions. For the 47 MeV/nucleon $^{64}\text{Zn} + ^{92}\text{Mo}$ we selected a range of midcentral collisions having charged particle and neutron multiplicities similar to those for the events selected for the 35 MeV/nucleon $^{64}\text{Zn} + ^{92}\text{Mo}$ reaction to have a comparable excitation energy.

For the selected events we carried out analyses using three source fits to the observed energy and angular distributions of the light charged particles. The assumed sources are the projectilelike fragment (PLF) source, the targetlike fragment (TLF) source and an intermediate velocity (IV) source [17–20]. As in the earlier work, the IV source typically has a source velocity very close to half of that of the projectile (i.e., that expected for nucleon-nucleon scattering). From these fits we obtained parameters describing the ejectile spectra and multiplicities that can be associated to the three different sources. Given the continuous dynamic evolution of the system, such source fits should be considered as providing only a schematic picture of the emission process. We have employed them to estimate the multiplicities and energy emission at each stage of the reaction.

For the four reactions studied, the parameters for emission of p , d , t , ^3He , and ^4He from the different sources, derived from the fits, follow the trends of earlier reported values at such projectile energies [10,17–20]. For each individual reaction system the IV source slope temperatures for p , d , t , ^3He , and ^4He are quite similar. They have values in the range of 11 to 16 MeV, characteristic of those for preequilibrium emission in this projectile energy range [10,17–20]. The slope parameters for the TLF sources are much lower, in the range of 4–6 MeV. For both sources the observed spectra result from a summation of the spectra of particles emitted over a range of time. Thus the observed slope temperature values are affected by the relative emission probabilities over that time period.

IV. EXCITATION ENERGY DETERMINATIONS

The masses and excitation energies of the hot nuclei which remain after the early (PLF and IV source) emission have been determined from the source fit parameters. The masses were obtained by subtracting, from the total entrance channel mass, the mass removed by projectile source and intermediate

TABLE I. Properties of the hot nuclei produced in midcentral collisions. Errors are estimated absolute uncertainties.

Reaction	A_{comp}	E^* (MeV/nucleon)	T_{HHe} (MeV)	T_{slope} (MeV)	ΔA_{evap}	$E^*/\Delta A$ (MeV/nucleon)
35 MeV/nucleon $^{64}\text{Zn} + ^{92}\text{Mo}$	96.4 ± 8.7	4.88 ± 0.49	5.93 ± 0.59	5.10 ± 0.50	38.7 ± 3.5	12.1 ± 1.7
35 MeV/nucleon $^{40}\text{Ar} + ^{112}\text{Sn}$	107 ± 9.6	4.98 ± 0.50	5.98 ± 0.60	5.80 ± 0.30	41.0 ± 3.7	13.0 ± 1.8
47 MeV/nucleon $^{64}\text{Zn} + ^{92}\text{Mo}$	85.4 ± 7.8	5.14 ± 0.51	5.60 ± 0.56	5.50 ± 0.03	35.5 ± 3.3	12.4 ± 1.8
55 MeV/nucleon $^{27}\text{Al} + ^{124}\text{Sn}$	114 ± 10	5.31 ± 0.53	6.00 ± 0.60	5.60 ± 0.10	44.5 ± 4.1	13.6 ± 1.9

source particles. These were determined from integrations of the source fits over 4π .

For each reaction system the excitation energy remaining in the TLF source was determined using calorimetric techniques. The data allow two different methods to make such a determination. The first is by subtraction, from the initial available energy, of the total energy (kinetic energy and Q value) removed by the PLF and IV sources and the kinetic energy of the primary remnant. For this purpose, the primary remnant kinetic energy was determined from the TLF source velocity and the mass not removed by the IV and projectile like sources. The second method consists of a reconstruction of the TLF excitation energy by using the information on the multiplicities and kinetic energies of light charged particles, neutrons, and intermediate mass fragments associated with the TLF source as follows:

$$E^* = \sum_i \bar{M}_{cp}(i) \bar{E}_{cp}(i) + \bar{M}_n \bar{E}_n + Q + E_\gamma, \quad (1)$$

where the sum extends over charged particle type i , $\bar{M}_{cp}(i)$ and \bar{M}_n are the average multiplicities of charged particles and neutrons, $\bar{E}_{cp}(i)$ and \bar{E}_n are their average kinetic energies, E_γ is the total energy of the emitted γ rays (estimated as 10 MeV), and Q is the Q value for the observed deexcitation starting from the primary TLF and assuming IMF masses consistent with the EPAX parameterization [21]. Some differences were observed in the results from the two different methods of excitation energy determination. These reflect inefficiencies in IMF detection resulting from incomplete coverage with Si detectors, energy thresholds, and emission at small laboratory angles not subtended by the detectors. As the two methods should agree we employed an iterative analysis to achieve convergence for the two different techniques, using the missing IMF multiplicity as a variable. For this purpose, the average masses and kinetic energies of these missing IMF were estimated from results of earlier experiments on some of the same systems [10,14,22].

A summary of the mass and excitation energy determinations for the TLF sources in these four systems is presented in Table I. The derived excitation energies range from 4.88 to 5.31 MeV/nucleon with estimated overall uncertainties of $\pm 10\%$. In the following discussion we take the derived excitation energies to be those of the equilibrated expanded systems [23,24], at the time corresponding to the latest particle

emission associated with the intermediate source and thus appropriate to the temperature determined at that time.

V. TEMPERATURES AT THE END OF PREEQUILIBRIUM EMISSION

We recently reported on the use of double isotope yield ratio measurements to determine the temperature evolution in intermediate-energy heavy-ion collisions [10]. At intermediate energies the observed spectral slope parameters derived from the source fits represent only some weighted average values as the observed spectra are convolutions of the spectra at different emission times. We have therefore employed isotope yields to determine the temperatures at the end of the preequilibrium emission stage of the reaction. Using the same techniques as in Ref. [10] we have determined the double isotope yield ratio temperatures as a function of ejectile velocity for the four different systems under consideration. The velocity employed is the ‘‘surface velocity,’’ V_{surf} , of the emitted particles, defined as the velocity of an emitted species at the nuclear surface, prior to acceleration in the Coulomb field [17]. The energy prior to Coulomb acceleration is obtained in our analysis by subtraction of the Coulomb barrier energy derived from the source fits. Because the early emitted light particle energies are strongly correlated with emission times, and the evaporative or secondary emission contributions to the spectra are primarily at the lower kinetic energies, the yields of higher energy particles are relatively uncontaminated by later emission processes.

The double isotope ratio temperatures employed are T_{HHe} , derived from the yields of d , t , ^3He , and ^4He clusters. To calibrate the time scale associated with our data we have used the results of AMD-V transport model calculations [9] to determine the relationship between calculated emission time and average ejected nucleon velocities for the different systems. The small charged ejectiles— d , t , ^3He , and ^4He , emitted at early times are treated as resulting from coalescence of the nucleons [10,13,14,17]. To focus on the earlier evolution of the system we selected such clusters emitted at midrapidity (i.e., at angles of 70 to 80 degrees in the IV source frame). In this way we attempted to isolate the emission associated with the IV source that occurs during the thermalization stage of the reaction. At midrapidity there is little contribution from

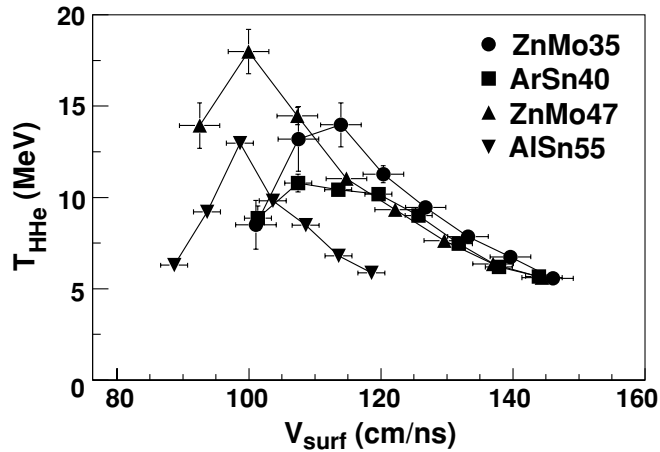


FIG. 1. Time evolution of the double isotope ratio temperature, T_{HHe} , for the four different reactions. Key is as follows: 35 MeV/nucleon $^{64}\text{Zn} + ^{92}\text{Mo}$ (red diamonds), 40 MeV/nucleon $^{40}\text{Ar} + ^{112}\text{Sn}$ (orange triangles), 55 MeV/nucleon $^{27}\text{Al} + ^{124}\text{Sn}$ (yellow circles), and 47 MeV/nucleon $^{64}\text{Zn} + ^{92}\text{Mo}$ (blue squares).

the PLF source remaining. There is, however, some observed contribution from the TLF source at low velocities in the IV source frame. In the following analysis yields assigned to the TLF source have been subtracted from the experimental yields.

As in Ref. [10], the AMD-V model calculations [8,9] indicate a significant slowing in the rate of kinetic energy change near a velocity of 3.5 cm/ns. This signals the end of the IV (or preequilibrium) emission stages and entry into the region of slower nuclear deexcitation modes (i.e., evaporation, fission, and/or fragmentation). At that point the sensitivity of the emission energy to time is significantly reduced. Therefore we take the temperature at the time corresponding to the velocity of 3.5 cm/ns to be that of the hot nucleus at the beginning of the final statistical emission stage.

We present, in Fig. 1, the double isotope ratio temperatures as a function of emission time. As time increases, each of the temperature evolution curves rises to a maximum and then decreases. Maximum temperatures of 10–15 MeV are observed at times in the range of 95 to 110 fm/c. After that the temperatures drop monotonically. Because the transport model calculations indicate that contributions from the late stage evaporation become dominant below $V_{\text{surf}} = 3.5$ cm/ns (see also Ref. [10]) we terminate the curves at the times corresponding to that velocity. We take these times to represent the end of the IV (or preequilibrium) emission stage. It is worth noting that the corresponding temperatures, presented in column 4 of Table I, are near 6 MeV and thus very similar to the limiting temperatures previously derived from a systematic investigation of caloric curve measurements [23] in this mass region.

The trends in Fig. 1 are very similar to those reported in Ref. [10] for the temperature evolution in the reactions of 26–47 MeV/nucleon ^{64}Zn projectiles with Ni, Mo, and Au targets. The possible interpretation of these trends is extensively discussed in that reference. It is concluded that the

data are consistent with chemical and thermal equilibration of the ensemble of events sampled, at least on a local basis.

If thermal and chemical equilibrium are achieved by the time of entry into the final fragmentation or evaporation phase of the reaction and the density at that point is not too high [25] an agreement between the thermal temperature and the double isotope ratio temperature T_{HHe} at that time can be expected. The TLF source fit slope parameters, T_{slope} for α particles are seen in column 5 of Table I to be slightly lower than the latest time T_{HHe} temperatures. This is not surprising because these T_{HHe} temperatures represent the temperature at the start of the deexcitation cascade, whereas the TLF source fits to the α spectra can be expected to return only an apparent temperature reflecting the entire evaporation and cooling history of the TLF source. In previous work [20,26,27] we have found that the slope parameters for the α -particle emission from the TLF source most closely approximates the initial thermal temperature of this source, reflecting the higher fraction of the α emission in the earlier part of the deexcitation cascade. The agreement between these thermal fit apparent temperatures and the late time chemical temperatures obtained from the isotope ratio temperatures, as presented in column 4 is quite reasonable given the associated uncertainties.

VI. DEEXCITATION CASCADES

If, in fact, the hot nuclei have achieved equilibration at very similar excitation energies and temperatures, this should be reflected in their deexcitation patterns. Figure 2 presents the hot nucleus masses, excitation energies, and T_{HHe} temperatures for the four different systems (in row 1 of the figure) and a comparison of average slope temperatures, multiplicities, and kinetic energies for $n, p, d, t, ^3\text{He}$, and ^4He emission during the TLF deexcitation. For each of the quantities presented in the figure, a dashed line representing the average values obtained for the 35 MeV/nucleon $^{64}\text{Zn} + ^{92}\text{Mo}$, 40 MeV/nucleon $^{40}\text{Ar} + ^{112}\text{Sn}$, and 47 MeV/nucleon $^{64}\text{Zn} + ^{92}\text{Mo}$ reactions (which lead to nuclei with similar N/Z ratios) is also shown. For each individual system, deviations from those averages are seen to be relatively small except for the enhanced neutron multiplicity for the 55 MeV/nucleon $^{27}\text{Al} + ^{124}\text{Sn}$ reaction, which is to be expected given the larger total excitation energy and significantly higher N/Z of the hot nucleus produced with this neutron rich target [12]. Because the total excitation energies do vary, we present, in column 6 of Table I, the total mass removed by TLF ejectiles and in column 7, the ratio of total excitation energy to total mass removed by the TLF ejectiles. This latter number is seen to be quite stable within experimental uncertainties. The average value, 12.8 ± 1.8 MeV, is close to values obtained in an early study of the energetics and deexcitation in reactions of 27 MeV/nucleon ^{40}Ar with Ag and Ho leading to somewhat heavier hot nuclei with similar excitation energies [28]. In that study, which detected heavy residues, equilibration and isotropy of emission was inferred from the residue velocity and angular distributions. In the present work, isotropy of emission from the TLF source is indicated by the success of that assumption in the source fitting process. Except for the expected additional favoring of neutron emission over

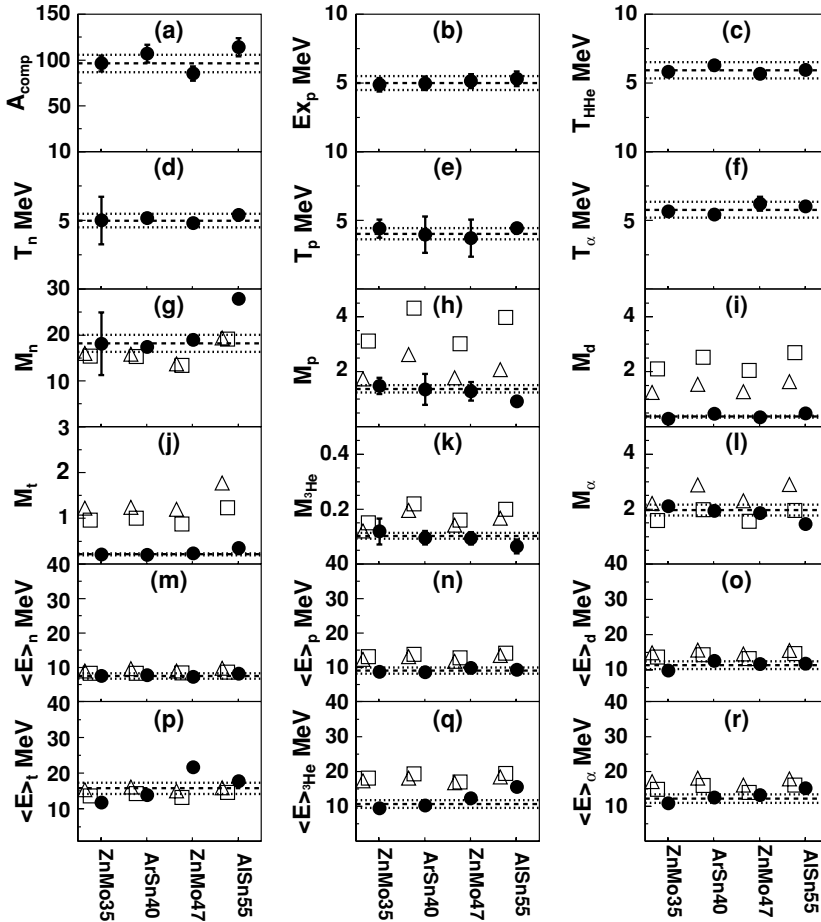


FIG. 2. Comparison of initial properties of the hot nuclei and deexcitation modes for the four different systems. (a) Masses of the de-exciting hot nuclei; (b) excitation energies of the hot nuclei; (c) double isotope temperatures, T_{HHe} ; (d)–(f) slope temperatures for n , p and t ; (g)–(l) multiplicities of n , p , d , t , ${}^3\text{He}$, and α ; (m)–(r) average kinetic energies of n , p , d , t , ${}^3\text{He}$, and α in the hot nucleus frame. Solid points represent the data for the four different systems. Open squares show the results of GEMINI calculations [29]. Open triangles show the results of SMM calculations [30].

charged particle emission for the reaction with the ${}^{124}\text{Sn}$ target, the very similar deexcitation patterns and energetics for the four hot nuclei that were produced in somewhat different dynamical conditions, is most easily understood as a reflection of statistical emission from very similar equilibrated hot nuclei.

It is interesting therefore to ask how the values in Fig. 2 compare with those calculated using current statistical model codes. For this purpose we have carried out calculations using both the GEMINI code [29] and the statistical multifragmentation model code (SMM) [30]. Except for an exploration of the effect of varying the level density parameter, a , these codes were used with normal default parameters and no attempt has been made to tailor them to the current data. For these highly excited systems the change in the multiplicities and average energies which results from varying the GEMINI code level density parameter was found to be rather small. The GEMINI results in Fig. 2 were obtained with a level density parameter, $a = A/9$. Yoshida *et al.* found this to be a reasonable average value in their study of neutron emission in the reactions of ${}^{40}\text{Ar} + {}^{92}\text{Mo}$ [12].

As is seen in that figure, the calculated relative values of the multiplicities and average energies for each system show trends quite similar to those of the experiments, suggesting that the statistical picture has some validity. However, the statistical model calculations systematically produce more $Z = 1$ ejectiles and fewer neutrons than have been observed

in the experiments. A similar underprediction of neutron emission is seen in Ref. [12]. In addition, except for the protons, the calculated average kinetic energies of the charged ejectiles are somewhat higher than the experimental values. Given that the dynamic calculations indicate that the initial hot deexciting nuclei produced in these collisions have more complicated shapes and density distributions than those assumed in the calculations it is perhaps not so surprising that some differences between the experimental results and the calculated results are observed.

VII. CONCLUSION

Establishing that equilibration has occurred in Fermi-energy collisions is difficult but remains an important prerequisite in determining the applicability of many of the techniques that have been utilized or proposed as tools to derive information on the nuclear equation of state at nonnormal densities [4–7]. In this article we have presented results of a Ghoshal-like experimental test of equilibration of medium mass hot composite nuclei produced in central collisions of 35 to 55 MeV/nucleon projectiles with medium mass targets. Although, in contrast to the low-energy experiments of Ghoshal, the present entrance channel mass asymmetries and energies differ significantly for the four

different cases studied and the masses of the final residues are less than half of the entrance channel masses, comparisons of the early temperature evolution and of the subsequent deexcitation patterns for the four systems indicate that very similar hot nuclei are indeed produced and that they decay in a very similar manner. Multiplicities and energies derived from statistical model calculations of the deexcitation of these hot nuclei show system to system trends similar to those of the experimental results but some quantitative differences in the competition between neutron and light charged particle emission. Overall, the results are most easily understood as a reflection of statistical emission from very

similar equilibrated hot nuclei. That such systems achieve equilibration is in agreement with the conclusions of a recent study in which evidence for equilibration was derived from observations of the temperature evolution in similar collisions [10].

ACKNOWLEDGMENTS

This work was supported by the United States Department of Energy under Grant DE-FG03-93ER40773 and by The Robert A. Welch Foundation under Grant A0330.

-
- [1] S. N. Ghoshal, *Phys. Rev.* **80**, 939 (1950).
 [2] N. Bohr, *Nature* **137**, 344 (1936).
 [3] J. Blatt and V. F. Weisskopf, *Theoretical Nuclear Physics* (John Wiley & Sons, Inc., New York, 1952).
 [4] E. Suraud, C. Gregoire, and B. Tamain, *Prog. Part. Nucl. Phys.* **23**, 357 (1989).
 [5] B. Tamain and D. Durand, University of Caen Report LPCC 96-16 (1996); and references therein.
 [6] P. Chomaz, *AIP Conference Proceedings*, **610**, 167 (2001).
 [7] Y. G. Ma *et al.*, nucl-ex/0410018, *Phys. Rev. C* in press (2005).
 [8] A. Ono, *Phys. Rev. C* **59**, 853 (1999).
 [9] R. Wada, T. Keutgen, K. Hagel, Y. G. Ma, J. Wang, M. Murray, L. Qin, P. Smith, J. B. Natowitz, R. Alfaro, J. Cibor, M. Cinausero, Y. ElMasri, D. Fabris, E. Fioretto, A. Keksis, S. Kowalski, M. Lunardon, A. Makeev, N. Marie, E. Martin, Z. Majka, A. Martinez-Davalos, A. Menchaca-Rocha, G. Nebbia, G. Prete, V. Rizzi, A. Ruangma, D. V. Shetty, G. Souliotis, P. Staszal, M. Veselsky, G. Viesti, E. M. Winchester, S. J. Yennello, W. Zipper, and A. Ono, *Phys. Rev. C* **69**, 044610 (2004).
 [10] J. Wang, R. Wada, T. Keutgen, K. Hagel, Y. G. Ma, M. Murray, L. Qin, A. Botvina, S. Kowalski, T. Materna, J. B. Natowitz, R. Alfaro, J. Cibor, M. Cinausero, Y. El Masri, D. Fabris, E. Fioretto, A. Keksis, M. Lunardon, A. Makeev, N. Marie, E. Martin, Z. Majka, A. Martinez-Davalos, A. Menchaca-Rocha, G. Nebbia, G. Prete, V. Rizzi, A. Ruangma, D. V. Shetty, G. Souliotis, P. Staszal, M. Veselsky, G. Viesti, E. M. Winchester, S. J. Yennello, W. Zipper, and A. Ono, *ArXiv Preprint nucl-ex/0408002* (2004), submitted to *Phys. Rev. C*.
 [11] I. Tilquin, Y. El Masri, M. Parlog, P. Collon, M. Hadri, T. Keutgen, J. Lehmann, P. Leleux, P. Lipnik, A. Ninane, F. Hanappe, G. Bizard, D. Durand, P. Mosrin, J. Peter, R. Rmbart, and B. Tamain, *Nucl. Instrum. Methods A* **365**, 446 (1995).
 [12] K. Yoshida, J. Kasagi, H. Hama, M. Sakurai, M. Kodama, K. Furutaka, K. Ieki, W. Galster, T. Kubo, M. Ishihara, and A. Galonsky, *Phys. Rev. C* **46**, 961 (1992).
 [13] J. Cibor, R. Wada, K. Hagel, M. Lunardon, N. Marie, R. Alfaro, W. Q. Shen, B. Xiao, Y. Zhao, J. Li, B. A. Li, M. Murray, J. B. Natowitz, Z. Majka, and P. Staszal, *Phys. Lett.* **B473**, 29 (2000).
 [14] K. Hagel, R. Wada, J. Cibor, M. Lunardon, N. Marie, R. Alfaro, W. Shen, B. Xiao, Y. Zhao, Z. Majka, P. Li, P. Staszal, B. A. Li, M. Murray, T. Keutgen, A. Bonasera, and J. B. Natowitz, *Phys. Rev. C* **62**, 034607 (2000).
 [15] J. Cibor *et al.*, in "Isospin Physics in Heavy-Ion Collisions at Intermediate Energies," edited by Bao-An Li, and W. Udo Schroeder NOVA Science Publishers, Inc., (New York, 2001).
 [16] Y. G. Ma, J. B. Natowitz, R. Wada, K. Hagel, J. Wang, T. Keutgen, Z. Majka, M. Murray, L. Qin, P. Smith, R. Alfaro, J. Cibor, M. Cinausero, Y. El Masri, D. Fabris, E. Fioretto, A. Keksis, M. Lunardon, A. Makeev, N. Marie, E. Martin, A. Martinez-Davalos, A. Menchaca-Rocha, G. Nebbia, G. Prete, V. Rizzi, A. Ruangma, D. V. Shetty, G. Souliotis, P. Staszal, M. Veselsky, G. Viesti, E. M. Winchester, and S. J. Yennello, nucl-ex/0410018, submitted to *Phys. Rev. C*.
 [17] T. C. Awes, G. Poggi, C. K. Gelbke, B. B. Back, B. G. Glagola, H. Breuer, and V. E. Viola, Jr., *Phys. Rev. C* **24**, 89 (1981).
 [18] T. C. Awes, G. Poggi, S. Saini, C. K. Gelbke, R. Legrain, and G. D. Westfall, *Phys. Lett.* **B103**, 417 (1981).
 [19] D. Prindle, A. Elmaani, C. Hyde-Wright, W. Jiang, A. A. Sonzogni, R. Vandenbosch, D. Bowman, G. Cron, P. Danielewicz, J. Dinius, W. Hsi, W.G. Lynch, C. Montoya, G. Peaslee, C. Schwarz, M. B. Tsang, C. Williams, R.T. de Souza, D. Fox, and T. Moore, *Phys. Rev. C* **57**, 1305 (1998).
 [20] R. Wada, D. Fabris, K. Hagel, G. Nebbia, Y. Lou, M. Gonin, J. B. Natowitz, R. Billerey, B. Cheynis, A. Demeyer, D. Drain, D. Guinet, C. Pastor, L. Vagneron, K. Zaid, J. Alarja, A. Giorni, D. Heuer, C. Morand, B. Viano, C. Mazur, C. Ngo, S. Leray, R. Lucas, M. Ribrag, and E. Tomasi, *Phys. Rev. C* **39**, 497 (1989).
 [21] K. Sümmerer and B. Blank, *Phys. Rev. C* **61**, 034607 (2000).
 [22] S. Kowalski *et al.*, work in progress.
 [23] J. B. Natowitz, R. Wada, K. Hagel, T. Keutgen, M. Murray, A. Makeev, L. Qin, P. Smith, and C. Hamilton, *Phys. Rev. C* **65**, 034618 (2002).
 [24] L. G. Sobotka, R. J. Charity, J. Töke, and W. U. Schröder, *Phys. Rev. Lett.* **93**, 132702 (2004).
 [25] Z. Majka, P. Staszal, J. Cibor, J. B. Natowitz, K. Hagel, J. Li, N. Mdeidayeh, R. Wada, and Y. Zhao, *Phys. Rev. C* **55**, 2991 (1997).
 [26] K. Hagel, D. Fabris, P. Gonthier, H. Ho, Y. Lou, Z. Majka, G. Mouchat, M. N. Nambodiri, J. B. Natowitz, G. Nebbia, R. P. Schmitt, G. Viesti, R. Wada, and B. Wilkins, *Nucl. Phys.* **A486**, 429 (1988).
 [27] M. Gonin, M. Gonin, L. Cooke, K. Hagel, Y. Lou, J. B. Natowitz, R. P. Schmitt, S. Shlomo, B. Srivastava, W. Turmel, H. Utsunomiya, R. Wada, G. Nardelli, G. Nebbia, G. Viesti,

- R. Zanon, B. Fornal, G. Prete, K. Niita, S. Hannuschke, P. Gonthier, and B. Wilkins, *Phys. Rev. C* **42**, 2125 (1990).
- [28] M. F. Rivet, B. Borderie, H. Gauvin, D. Gardes, C. Cabot, F. Hanape, and J. Peter, *Phys. Rev. C* **34**, 1282 (1986).
- [29] R. J. Charity *et al.*, *Nucl. Phys.* **A483**, 371 (1988), <http://www.chemistry.wustl.edu/faculty/charity.html>.
- [30] J. P. Bondorf, A. S. Botvina, A. S. Iljinov, I. N. Mishustin, and K. Sneppen, *Phys. Rept.* **257**, 133 (1995); A. Botvina (private communication).